Intrinsic Nature of the Excess Electron Distribution at the $TiO_2(110)$ Surface

P. Krüger,[1,*] J. Jupille,[2] S. Bourgeois,[1] B. Domenichini,[1] A. Verdini,[3] L. Floreano,[3] and A. Morgante[3,4]

[1]*ICB, UMR 6303 CNRS-Université de Bourgogne, BP 47870, F-21078 Dijon, France*

[2]*Institut des NanoSciences de Paris, UPMC and CNRS, Campus de Jussieu, F-75252 Paris, France*

[3]*CNR-IOM, Laboratorio TASC, Basovizza, SS14, km 163.5, I-34149 Trieste, Italy*

[4]*Dipartimento di Fisica, Università di Trieste, via Alfonso Valerio 2, I-34127 Trieste, Italy*

(Received 25 January 2012; published 20 March 2012)

The gap state that appears upon reduction of TiO_2 plays a key role in many of titania's interesting properties but its origin and spatial localization have remained unclear. In the present work, the $TiO_2(110)$ surface is reduced in a chemically controlled way by sodium adsorption. By means of resonant photoelectron diffraction, excess electrons are shown to be distributed mainly on subsurface Ti sites strikingly similar to the defective $TiO_2(110)$ surface, while any significant contribution from interstitial Ti ions is discarded. In agreement with first principles calculations, these findings demonstrate that the distribution of the band gap charge is an intrinsic property of $TiO_2(110)$, independent of the way excess electrons are produced.

DOI: 10.1103/PhysRevLett.108.126803 PACS numbers: 73.20.Hb, 68.35.Dv, 79.60.−i

Titanium dioxide, an inert insulator in stoichiometric form, can be easily reduced into an *n*-type semiconductor TiO_{2-x} with many technologically relevant properties, including photocatalysis [1,2], chemical reactivity [3,4], and electrical conductivity [3]. Formally associated with the transformation of Ti^{4+} to Ti^{3+} ions, reduction of titania results in excess electrons that populate localized Ti $3d$ states in the band gap [1], giving rise to core-level shifts [5], changes in Auger line shapes [6], and a characteristic signature in electron paramagnetic resonance [7]. Despite a large number of experimental and theoretical studies, mainly focused on the archetypal $TiO_2(110)$ [3], a clear picture of the reduced surface has not been found to date. Puzzling issues are the surface or subsurface distribution of excess charges and the lattice or interstitial nature of the Ti^{3+} ions. In the classical oxygen-vacancy picture [8,9] of the rutile $TiO_2(110)$ surface, excess electrons originate from the vacancies created by the removal of bridging oxygen atoms (O_b-vac) and give rise to Ti $3d^1$ states on the surrounding Ti ions [9–11]. This view was contradicted by two recent experimental studies in which the Ti interstitial atoms (Ti_{int}) were attributed a main role in the band gap state [12,13]. According to Wendt *et al.* [12] the Ti $3d^1$ gap state mainly stems from Ti_{int}, since it was found hardly sensitive to the filling of O_b-vac by hydroxyl groups. In a different way, on the basis of a counting of O_b-vac by STM combined with a hybrid HSE06 approach, Papageorgiou *et al.* [13] postulated that excess electrons originate from both O_b-vac and Ti_{int} that stay close to the surface. Regarding the localization of Ti^{3+} ions, theory is far from consensus. Localized states in wide band gap oxides remain a challenge for first principles theory [4,14] and so the choice of the appropriate approach is the first issue in numerical simulations. In contrast to density functional theory (DFT), the DFT + U scheme [4] and DFT-Hartree-Fock hybrid functionals [14] include self-interaction corrections and are therefore expected to describe localized band gap states better than pure DFT. However, even similar functionals yield conflicting results. According to the hybrid B3LYP functional, known for improving the determination of gap widths [15], unpaired electrons are trapped on nonequivalent fivefold and sixfold coordinated surface Ti sites next to O_b-vac [14]. At variance, the hybrid HSE06 functional suggests electron localization on subsurface sites beneath O_b-vac [13]. DFT + U approaches favor charges in subsurface for low U values (< 4 eV) [16] or low concentration [17] and predict an occupancy of surface atomic sites for higher U values [16] or higher concentration [17]. The case is made even more complex by the large number of defect energy levels calculated for rutile [18] and anatase [19], and by the extreme sensitivity of titania surfaces to details of their history [12,20,21]. Unquestionably, a clear and generally accepted picture of the origin and nature of excess electrons at the rutile surface has not been found yet.

A previous study of a defective $TiO_2(110)$ surface has demonstrated the unique capability of resonant photoelectron diffraction (RPED) to map out the spatial distribution of band gap states [22] and has shown that excess electrons mostly occupy subsurface Ti sites [23–25]. However, these conclusions were challenged by the suggestion that Ti_{int} plays a dominant role in the creation of near surface excess charge [12,13]. Note that RPED experiments can discriminate between Ti lattice and interstitial sites provided the latter are close enough to the surface, as in the model of Wendt *et al.* [12,26]. Ti_{int} defects in deeper layers, which were considered by Papageorgiou *et al.* [13], are not directly probed by RPED. However, extra electrons coming from deep Ti_{int} are expected to strongly affect the excess

charge distribution [13] and would thus lead to a different RPED signature than O_b-vac.

Here we propose a new way to check the contribution of Ti_{int} ions in the defective $TiO_2(110)$ surface. It consists in comparing the excess electron distribution of the defective surface where Ti_{int} is one of the two possible defect types, with that of a stoichiometric surface which is electron doped in a controlled way by alkali metal deposition [23,27]. The crucial point is that in the latter system, the presence of Ti_{int} can be ruled out. The system chosen herein is $Na/TiO_2(110)$ because of its known geometry [28]. Apart from a slight change in bond relaxation, sodium adatoms do not perturb the rutile lattice [23]. In the submonolayer range, independently of coverage, Na adsorbs on a defined site without breaking Ti-O bonds, as was shown by concurrent numerical simulations [23] and experiments [28]. The excess charge distribution of this system has been predicted to be comparable to that arising from direct injection of excess electrons at the rutile surface [23].

The $TiO_2(110)$ surface has been prepared by argon sputtering (2.5 keV, 20 min) and annealing (970 K) in conditions known to give rise to (1×1) surfaces and to reduce the intensity of the 3d gap state [20]. Figure 1(a) shows the valence band photoemission spectra recorded with 462 eV photons at the maximum of the Ti-$L2$-edge resonance [6]. The x-ray beam impinged at grazing incidence with light polarization normal to the surface. As checked in resonant conditions, the gap state intensity

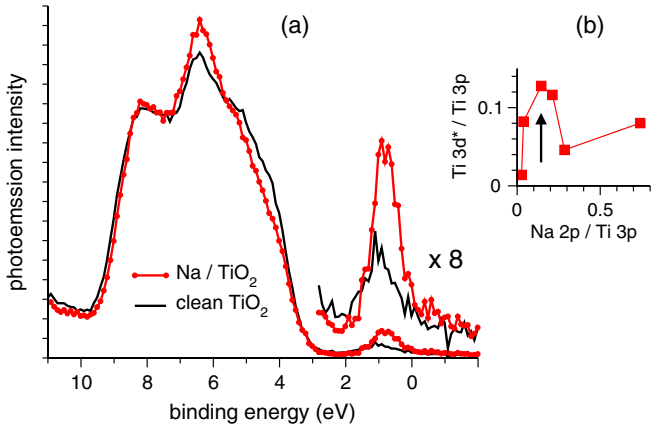

FIG. 1 (color online). Resonant photoemission spectra of $Na/TiO_2(110)$. (a) Valence band photoemission spectra of the $TiO_2(110)$ surface at the Ti-$L2$ resonance ($h\nu = 462$ eV) before (black line) and after Na deposition (red line with circles). The two spectra have been aligned at the valence band maximum. (b) Photoemission intensity variation of the Na-induced gap state (Ti-3d^* = difference of gap state intensity after and before Na deposition) as a function of Na coverage as estimated by the Na-2p intensity. Ti-3d^* and Na-2p intensities have been normalized to the Ti-3p line. Na-2p and Ti-3p have been measured off resonance at 150 eV photon chosen for maximum Na sensitivity. The arrow indicates the coverage used in the photoelectron diffraction experiment [Fig. 2(a)].

was minimized by exposure to oxygen at temperature <330 K. Great care was taken in this operation. Sodium was then deposited to maximize the sodium-induced gap state occupation [Fig. 1(b)]. Upon Na adsorption, as seen in Fig. 1(a), the gap state intensity increased by a factor of 2.5–3. Thus the majority of excess electrons was due to charge transfer from Na. As in previous experiments on the defective surface [22], RPED was measured for photoelectrons from the gap state at the Ti-$L2$ resonance ($h\nu = 462$ eV). The photoemission intensity I of the gap state was recorded as a function of polar angle θ and azimuthal angle ϕ. For the analysis we consider the azimuthal anisotropy function $\chi(\theta, \phi) = [I(\theta, \phi) - I_0(\theta)]/I_0(\theta)$ where $I_0(\theta)$ denotes the ϕ average of $I(\theta, \phi)$ and represents the intensity without diffraction effects and instrumental contributions. A stereographic χ plot is called a RPED pattern. The difference between two patterns χ_a and χ_b is measured through the R factor $R_{ab} = \int(\chi_a - \chi_b)^2 d\Omega / \int(\chi_a^2 + \chi_b^2) d\Omega$, where Ω is the solid angle. Integration runs over the whole experimental θ range from 0° to 65°. $R = 0$ and $R = 1$ correspond to identical and uncorrelated data sets, respectively.

The experimental RPED pattern of $Na/TiO_2(110)$ is shown in Fig. 2(a). Its striking similarity with the defective $TiO_2(110)$ pattern [22] [Fig. 2(b)] is consistent with the small R factor obtained between these two patterns (0.152). Since a RPED pattern from the gap state is a fingerprint of the local environment of the Ti^{3+} ions, this comparison immediately suggests that excess electrons are located on essentially the same Ti sites whether created by Na adsorption or by surface defects.

A quantitative description of the excess charge distribution can be achieved by a least-squares fit of a theoretical pattern to the experimental one [22]. The band gap state intensity photoemitted by some site Ti(n) is assumed proportional to the amount of excess charge on that site. The theoretical pattern is computed from a weighted sum of photoemission intensities from the different emitter sites Ti(n). The relative weights are obtained by minimizing the R factor between theory and experiment. Patterns for the Ti sites in the first three layers of the Na-covered surface (Fig. 2, panels 1–6) have been obtained by multiple scattering cluster calculations [29]. The optimized simulated pattern and the corresponding location of excess charges are shown in Figs. 2(c) and 3(a), respectively. Site Ti3 dominates with a weight close to half, followed by Ti5 and Ti1. Sites Ti2, Ti4, and Ti6 have zero weight. For direct comparison, the RPED patterns of defective TiO_2 [22] have been reanalyzed here using the same integration range and cluster size as for Na/TiO_2 (with full investigation of the third layer emitters Ti5 and Ti6). Beyond the visual observation and the small relative R factor between patterns 2(a) and 2(b), least-square fits operated on equal basis directly prove that the distribution of excess electrons over Ti lattice sites is very similar for the defective and the Na-covered surface [Figs. 3(a) and 3(b)].

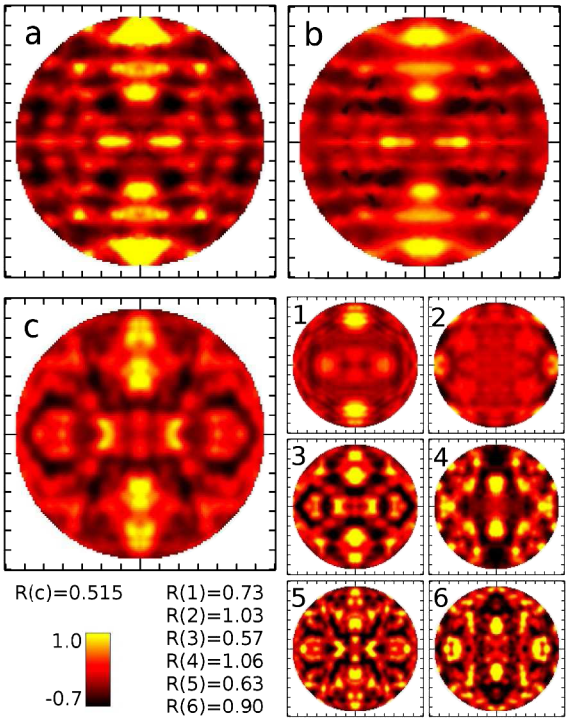

FIG. 2 (color online). Resonant photoelectron diffraction patterns from the band gap state. The projection of the patterns $\chi(\theta, \phi)$ is linear in θ with the surface normal ($\theta = 0$) in the center. Ticks are drawn every 10°. $\phi = 0$ ($\phi = 90°$) is found at 3 o'clock (12 o'clock) and corresponds to the [1–10] ([001]) direction. (a) Experimental pattern of $Na/TiO_2(110)$. (b) Experimental pattern of defective $TiO_2(110)$ (adapted from Ref. [22]). (c) Calculated best fit pattern of $Na/TiO_2(110)$ with weights as given in Fig. 3(a). Panels 1–6: Calculated patterns for Ti-3d emission from sites Ti 1–6 (see Fig. 3 for the atomic positions). The R factors between experimental (a) and calculated patterns [(c), 1–6] are indicated.

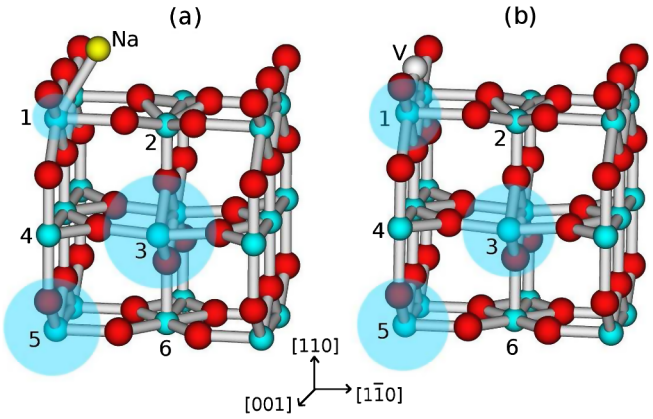

FIG. 3 (color online). Location of excess charge. (a) $Na/TiO_2(110)$. (b) Defective $TiO_2(110)$. The small balls are Ti (blue or light gray), O (red or dark gray), and Na atoms and V denotes an O vacancy. The bigger, shaded spheres symbolize the excess charge located on a given type of Ti site with diameters proportional to the amount of charge. The relative weights are (a) Ti1 18%, Ti3 44%, Ti5 38%. (b) Ti1 28%, Ti3 36%, Ti5 36%. Ti2, Ti4, and Ti6 have zero weight.

The almost perfect similarity between the two experimental patterns [Figs. 2(a) and 2(b)] provides a pivotal piece of information on the nature of the Ti^{3+} ions. In the model used to fit the RPED data, it has implicitly been assumed that all Ti^{3+} ions are on Ti lattice sites. The possibility that a substantial fraction of Ti^{3+} ions are on Ti_{int} sites, can indeed be excluded by a simple visual comparison of the RPED patterns of the Na-covered [Fig. 2(a)] and of the defective surface [Fig. 2(b)]. In fact, within a simple ionic model, each Ti_{int} can reduce three other Ti atoms, giving four Ti^{3+} ions in total. Note that interstitial Ti atoms are expected to carry some excess charge since, on the basis of first principles calculations, among the four excess electrons that each Ti_{int} defect produces, at least one is expected to stay on the interstitial site [30]. If it is assumed that Ti_{int} is the majority defect type, then Ti_{int} would carry about $1/4$ of the excess charge of the defective surface. For the Na-covered surface, where the band gap state is populated and increased by a factor of 2.5–3 [see Fig. 1(a)], the fraction of charge on Ti_{int} would go down by the same factor, i.e., to about 10%. The RPED pattern recorded on the Na-covered surface would then strongly differ from that of the defective surface. Thus the close similarity of the two patterns [Figs. 2(a) and 2(b)] directly demonstrates that Ti_{int} cannot be the dominant defect type at the $TiO_2(110)$ surface. The possible occurrence of Ti_{int} in deep ($>$ 3rd) layers cannot be probed directly by RPED because of the limited photoelectron escape depth. However, if such defects are present and a part of their charge is transferred to the near surface layers (as suggested in Ref. [13]) then we can conclude that this charge is distributed over the same Ti sites as the excess charge from O_b-vac or Na adatoms. Finally, the absence of Ti_{int} in the first three surface layers was checked quantitatively by simulations. RPED patterns corresponding to Ti_{int} emission were calculated for all interstitial sites in the first and second interlayers (Fig. 4). The calculated patterns strongly differ from experiment [defective TiO_2, Fig. 2(b)] with R factors close to 1. When any of the four interstitial sites was included in the R-factor minimization, its optimum weight was found to be zero. Therefore, the suggestion that Ti interstitial atoms play a central role in the near surface excess electron distribution [12,13,26] is not supported by the present data. Instead, the classical picture [8,9] is confirmed: excess electrons at $TiO_2(110)$ are due to oxygen vacancies and the band gap state is associated with Ti^{3+} ions on lattice sites.

The location of excess electrons on the subsurface Ti lattice sites qualitatively corresponds to DFT predictions of Albaret *et al.* [23] and Deskins *et al.* [25], except that Ref. [25] finds no excess charge at the Ti1 site. Moreover, the experimental finding that bridging oxygen vacancies and sodium adsorption lead to similar excess charge distributions is consistent with comparative calculations for excess electrons on bare $TiO_2(110)$ and either H-doped, hydroxylated [14,24] or Na-doped surfaces [23].

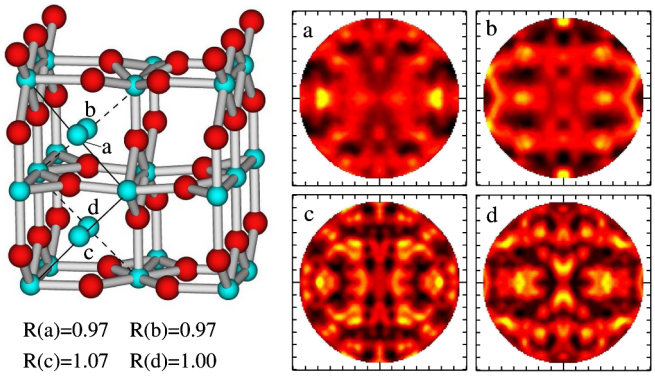

FIG. 4 (color online). Calculated photoelectron diffraction patterns for Ti interstitial sites. Left: The four nonequivalent Ti interstitial sites [labeled (a), (b), (c), (d)] in the first two interlayers of TiO_2(110). Right: Calculated photoelectron diffraction patterns for Ti-3*d* emission from these sites. The color scale is the same as in Fig. 2. The *R* factors with respect to the experimental pattern of the defective surface [Fig. 2(b)] are indicated.

The agreement with theory demonstrates that the localization of the excess electrons is dictated by the electrostatics, i.e., by the variation of the Hartree potential between the different Ti lattice sites [23,25]. The variation results from a combination of surface lattice relaxations [23] and polaronic distortions, with weak, if any, dependence on the way excess electrons are produced. Finally, the convergence between the present experiments and theory [23,25] proves the relevance of the comparison with calculations performed at 0 K [31]. Data recorded at 300 K are expected to show some broadening of the excess charge to the neighbors of the lowest energy sites [24,25], which does not, however, change the main interpretations gained at $T = 0$ K. The close similarity between excess electron distributions of different origin, as analyzed by photoelectron diffraction, leads to a unique model of the reduced TiO_2(110) surface with two main aspects. First, excess electrons mainly occupy subsurface lattice Ti atoms of the second and third layer. No evidence could be found of any significant contribution from interstitial titanium ions, even from deeper layers. Consequently, the defect state at the reduced TiO_2(110) is due to oxygen vacancies and their distribution stems from electrostatics. Second, the charge distribution of the band gap state is essentially an intrinsic property of the TiO_2(110) surface, because largely independent of the way excess electrons are created. The unified picture of excess electrons that emerges from the present work has far-reaching consequences for the understanding of surface chemistry of titania and the corresponding theoretical modeling.

*pkruger@u-bourgogne.fr

[1] T. L. Thompson and J. T. Yates, Jr., Chem. Rev. **106**, 4428 (2006).
[2] M. A. Henderson, Surf. Sci. Rep. **66**, 185 (2011).
[3] U. Diebold, Surf. Sci. Rep. **48**, 53 (2003).
[4] M. V. Ganduglia-Pirovano, A. Hofmann, and J. Sauer, Surf. Sci. Rep. **62**, 219 (2007).
[5] J. T. Mayer, U. Diebold, T. E. Madey, and E. Garfunkel, J. Electron Spectrosc. Relat. Phenom. **73**, 1 (1995).
[6] P. Le Fèvre, J. Danger, H. Magnan, D. Chandesris, J. Jupille, S. Bourgeois, M.-A. Arrio, R. Gotter, A. Verdini, and A. Morgante, Phys. Rev. B **69**, 155421 (2004).
[7] T. Sekiya, T. Yagisawa, N. Kamiya, D. Das Mulmi, S. Kurita, Y. Murakami, and T. Kodaira, J. Phys. Soc. Jpn. **73**, 703 (2004).
[8] V. E. Henrich, Rep. Prog. Phys. **48**, 1481 (1985).
[9] C. M. Yim, C. L. Pang, and G. Thornton, Phys. Rev. Lett. **104**, 036806 (2010).
[10] Z. Zhang, S.-P. Jeng, and V. E. Henrich, Phys. Rev. B **43**, 12004 (1991).
[11] R. Heise, R. Courths, and S. Witzel, Solid State Commun. **84**, 599 (1992).
[12] S. Wendt *et al.*, Science **320**, 1755 (2008).
[13] A. C. Papageorgiou, N. S. Beglitis, C. L. Pang, G. Teobaldi, G. Cabailh, Q. Chen, A. J. Fisher, W. A. Hofer, and G. Thornton, Proc. Natl. Acad. Sci. U.S.A. **107**, 2391 (2010).
[14] C. Di Valentin, G. Pacchioni, and A. Selloni, Phys. Rev. Lett. **97**, 166803 (2006).
[15] J. Muscat, A. Wander, and N. M. Harrison, Chem. Phys. Lett. **342**, 397 (2001).
[16] B. J. Morgan and G. W. Watson, J. Phys. Chem. C **113**, 7322 (2009).
[17] C. J. Calzado, N. C. Hernández, and J. Fdez. Sanz, Phys. Rev. B **77**, 045118 (2008).
[18] A. K. Ghosh, F. G. Wakim, and R. R. Addiss, Jr., Phys. Rev. **184**, 979 (1969).
[19] C. Di Valentin, G. Pacchioni, and A. Selloni, J. Phys. Chem. C **113**, 20543 (2009).
[20] O. Bikondoa, C. L. Pang, R. Ithnin, C. A. Muryn, H. Onishi, and G. Thornton, Nature Mater. **5**, 189 (2006).
[21] M. Nolan, S. D. Elliott , J. S. Mulley, R. A. Bennett, M. Basham, and P. Mulheran, Phys. Rev. B **77**, 235424 (2008).
[22] P. Krüger *et al.*, Phys. Rev. Lett. **100**, 055501 (2008).
[23] T. Albaret, F. Finocchi, C. Noguera, and A. De Vita, Phys. Rev. B **65**, 035402 (2001).
[24] N. A. Deskins, R. Rousseau, and M. Dupuis, J. Phys. Chem. C **113**, 14583 (2009).
[25] N. A. Deskins, R. Rousseau, and M. Dupuis, J. Phys. Chem. C **115**, 7562 (2011).
[26] S. Wendt, R. Bechstein, S. Porsgaard, E. Lira, J. Ø. Hansen, P. Huo, Z. Li, B. Hammer, and F. Besenbacher, Phys. Rev. Lett. **104**, 259703 (2010).
[27] H. Onishi, T. Aruga, C. Egawa, and Y. Iwasawa, Surf. Sci. **199**, 54 (1988).
[28] P. Lagarde, A.-M. Flank, R. J. Prado, S. Bourgeois, and J. Jupille, Surf. Sci. **553**, 115 (2004)
[29] See Supplemental Material at http://link.aps.org/supplemental/10.1103/PhysRevLett.108.126803 for details of the cluster calculations and the *R* factor analysis.
[30] E. Cho *et al.*, Phys. Rev. B **73**, 193202 (2006).
[31] E. Finazzi, C. Di Valentin, and G. Pacchioni, J. Phys. Chem. C **113**, 3382 (2009).